Roller Bearing Slip and Skidding Damage

B. A. Tassone*
SKF Industries, Inc., King of Prussia, Pa.

Currently main shaft bearings are running at DN values in excess of two million. Within the next decade, it is reasonable to consider bearings operating at DN values of three million and higher. With slip being the primary parameter correlated to failure, it will become more troublesome at the higher DN values. Slip occurs in a cylindrical roller bearing when the radial load is inadequate to develop a frictional (tractional) drive force between rolling elements and rotating raceway to overcome drag forces. In order to predict the occurrence and magnitude of slip, an analytical method was developed to determine the cage speed through a series of force and torque balances. When excessive slip is predicted, there are several bearing designs that can be used to minimize it. However, the most successful has been to increase the applied load on the bearing with an "out-of-round" bearing which can have either a bilobe or trilobe. A main shaft bearing used in a particular helicopter engine had been a continued source of trouble. Although several bearing designs and materials were evaluated, the elliptical bearing was the most significant in reducing slip and skid damage.

Introduction

IN most cylindrical roller bearing applications, the shaft speed is relatively slow and radial loads are sufficiently high to assure rolling contact between the loaded rollers and the rotating raceway. The normal mode of failure in these types of applications with adequate lubrication is spalling fatigue. However, in jet engine main-shaft roller bearings, the operating conditions are normally just the opposite. The speeds are extremely high with very light external loading. Most frequently, surface distress arising under conditions of slip is the prime cause of failure. At this time main shaft bearings are running at DN (D is bearing bore in millimeters and N is shaft speed in rpm) values in excess of two million. Within the next decade it is reasonable to consider bearings operating at a DN value of three million and perhaps even higher. With slip being the primary parameter correlated to failure of current main shaft roller bearings, it will become more troublesome at the higher DN values. Therefore, a firm understanding of slip is essential for the successful operation of roller bearings to meet these future requirements.

Since skidding damage will be an important factor in the bearing design requirement for future bearings to meet the higher DN values, the intent of this paper is to define what is slip, how to recognize surfaces damaged by skidding and describe bearing designs that have proven to reduce slip and skid damage. Also included is a unique slip problem in a helicopter engine which was corrected with the use of an elliptical bearing design.

Difference Between Slip and Skid Damage

Before proceeding further, a distinction should be made between two words which are unfortunately used interchangeably, slip and skid damage. Slip is the relative difference in velocity between components which should be rolling; i.e., which have the same surface velocities. Under ideal conditions a rolling bearing should act as a planetary system with pure rolling at all surfaces. It is possible to have slip without resulting in surface damage. However, if damage does occur to the surfaces when slip is present, then this damage is more properly defined as skid damage or skid marking. Therefore, in order to have skid damage, slip must be present but it is not necessary that damage will always occur in the presence of slip. Neither can it be said that slip only is sufficient to cause skid damage. Other factors that should be considered are a vibrating shaft or an alternating load. This condition can produce a force that will break through the lubricant film and possibly result in skidding damage. Ideal lubrication of a rolling bearing occurs when a complete film of oil separates the rolling elements and the rings so that there is no metal to metal contact between the rolling elements and rings.

When two bodies close to each other and rotating at the same velocity roll on each other, the surfaces entrain lubricant which is squeezed into the narrowing gap between them, creating a film. Unfortunately, the film is sensitive to heat which can come from either an external source or internal friction. In pure rolling, the friction heat is very small but considerable heat is developed in other than pure rolling. As the lubricant is heated, the loss of viscosity reduces the film thickness. If the heating is intense enough, the film will become so thin that it will no longer separate the surfaces resulting in metal to metal contact.

Slip

Slip occurs in a cylindrical roller bearing when the radial load is inadequate to develop a frictional (tractional) drive force between rolling elements and rotating raceway to overcome drag. Referring to the roller bearing sketch in Fig. 1, the drag force is the sum of: a) friction at the nonrotating raceway contacts due to centrifugal force on the rolling elements as well as applied loads; b) friction between the rollers and cage; c) viscous losses in the lubricant; and d) friction between cage and outer ring guiding lands.

At high speed, outer ring expansion from centrifugal loading is usually greater than centrifugal expansion of

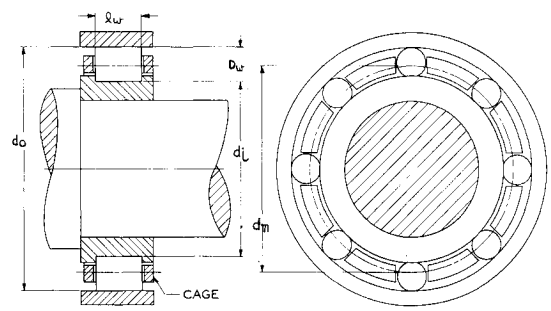

Fig. 1 Cylindrical roller bearing.

Received August 12, 1974; revision received February 21, 1975.
Index category: Aircraft Subsystem Design.
*Senior Application Engineer, Technology Center.

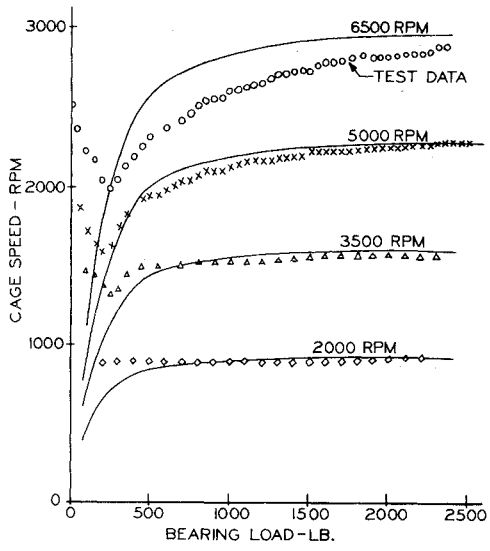

Fig. 2 Cage speed vs load and inner ring speed for a cylindrical roller bearing lubricant-diester type according to MIL-L-7808.

the inner ring, tending to increase clearance and thus reduce the number of rollers contacting the inner race with a load difference between inner and outer ring. There is a tendency for the drag forces to exceed the driving forces, thus, the cage must rotate at a speed somewhat less than pure rolling speed. This speed is defined as: cage slip = $[1 - (N_c/N_{cr})] \times 100$, where N_c is the cage speed and N_{cr} is the cage speed in pure rolling.

In pure rolling, the speed of the contact point traveling over the circumference of the rolling element is equal to the circumferential speed of the contact over the raceway. As the cage and rolling elements rotate around the bearing axis, the circumferential speed of the cage at the pitch circle can be expressed in equation form

$$v_c = 2\pi V_m N_c = v_i + v_0/2$$

where: V_c = cage velocity mm/sec.; V_m = pitch radius, mm.; d_m = pitch diam., mm.; D_w = roller diam., mm.; N_c = cage speed, rpm; V_i = inner ring velocity, mm/sec.; V_o = outer ring velocity, mm/sec.; N_i = inner ring speed, rpm; and N_o = outer ring speed, rpm.

Since

$$r_i = (d_m - D_w/2,\ r_0 = d_m + D_w/2$$

then

$$N_c = 1/2\ N_i[1 - (D_w/d_m)] + 1/2 N_0[1 + (D_w/d_m)]$$

As can be seen with inner-ring rotation and a stationary outer ring, the cage speed is always less than one half the inner-ring speed. For outer-ring rotation with a stationary inner ring, the cage speed is always greater than one half the outer-ring speed. Since drag forces exist, the cage speed is usually different from that calculated using pure rolling equations. This means that contact velocity on the rolling elements and rotating raceway are not equal and slip exists.

In order to predict the occurrence and magnitude of slip, an analytical method was developed to determine the cage speed through a series of force and torque balances including the fluid frictional drag forces at the contacts, the cage drag loads, and the normal forces due to centrifugal and external loading. This analysis was presented in detail by Harris.[1] An illustration of this method comparing the analytical data vs experimental data is shown in Fig. 2. The solid lines represent the predicted cage speed as compared to measured cage speeds shown by dots. The shape of the analytical curves closely approximates the test data in the higher load range. As previously mentioned, the terms skid damage and skid marking have been applied to a type of surface damage found in aircraft engine bearings.

Skid Damage

A description of skid marking is given by providing a series of photomicrographs at various magnifications which show the physical appearance of the skid markings as compared to areas which do not contain skid markings. Visually, the markings are dull regions which make them contrast strongly with nonskid marked regions which have a bright, shiny appearance. When examined with the light microscope, skid marked areas appear as micropitted regions. Optical micrographs comparing unrun, skid marked and nonskid marked surfaces on inner ring are shown in Fig. 3.

At the boundary of the skid-damaged areas, the skid marks trail off in a series of "streamers." This is shown in Fig. 4, where both skid markings and the smooth nonskid marked areas can be seen. The "streamers" on the skid markings follow the fine finishing marks on the bearings although this is not obvious in the photomicrograph of Fig. 4.

Because of the difficulties in obtaining good lighting conditions on the sample to illustrate this point, a plastic replica was made of such an area and photographed by transmitted light which provides a more even illumination

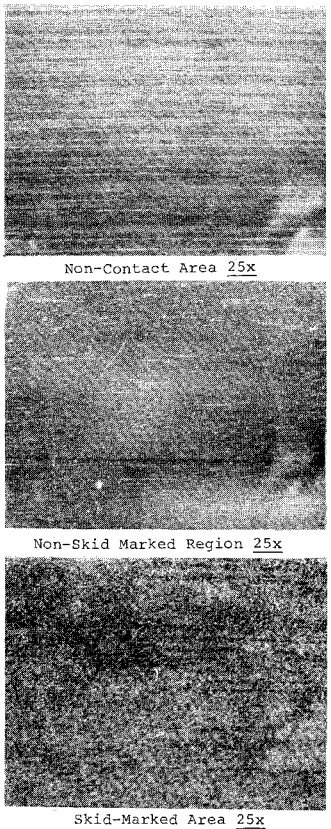

Fig. 3 Micrographs of bearing surfaces.

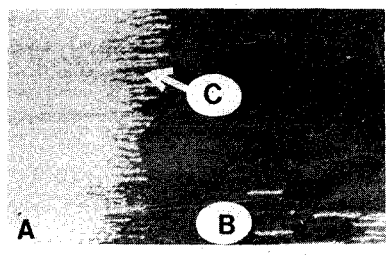

Fig. 4 Boundary of skid marked region.

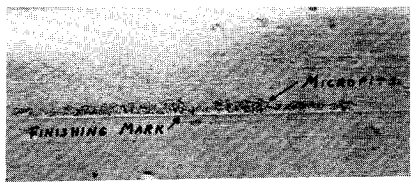

Fig. 5 Photomicrograph of replica of the skid marked area.

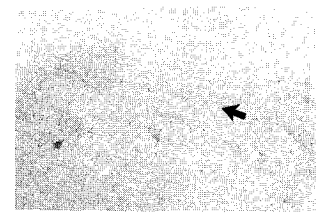

Fig. 7 Replica electron micrograph of a noncontact area of an inner ring.

and shows the micropits of the skid marks clustered around a surface scratch. This is illustrated in Fig. 5. In order to obtain a quantitative description of the surface condition and determine the depth of the micropits in the skid marked areas, surface profile tracings were taken across skid marked and nonskid marked areas. The talysurf traces are shown in Fig. 6 where chart "A" shows an uncontacted area of the inner ring and the point where the skid markings begin. The surface finish in the noncontact area is very smooth and regular while the skid marked area is a region filled with micropits which are from material transfer. The micropits vary considerably in depth, the deepest being shown as approximately 100 μin. and in some places the material rises above the original surface while the smooth areas in the center are unaffected. The large difference in horizontal and vertical magnifications of the talysurf trace makes it difficult to grasp the proper width to depth ratio of the micropits. Because of the low magnification in the horizontal direction, it is also difficult to establish the extent of pitting compared to the amount of original surface remaining in the skid marked regions. The replica electron micrographs (to be discussed) give a better picture of the extent of the surface damage.

Chart "B" in Fig. 6 shows a trace across the boundary between a skid marked area and one of the smooth patches which is surrounded by skid markings. There is no obvious difference between the surface finish on the unrun area and that of the smooth patch in the center of the ring. The shallow depth of focus of light microscopes limits their usefulness in studying fractured or irregular surfaces at higher magnifications. The high resolving power of electron microscopes combined with their great depth of focus makes them useful in studying rough and fractured surfaces. Since the skid marked areas contain many relatively deep micropits, replica electron microscope was used to examine the skid markings at high magnifications (above 1000 diam.).

Replicas were made of noncontact areas, skid marked areas, and the smooth patches in the contact areas. A typical electron micrograph of a noncontact area is shown in Fig. 7. This is a high magnification picture of the surface and the only visible features are some fine finishing marks on the bearing surface. Figure 8 is an electron micrograph of a typical skid marked area. The micropits are the irregularly shaped regions marked "A" while the original surface can be identified by the finishing marks such as those seen at "B." Close examination of the micropits shows that each is a small volume of material spalled from the surface. There is no evidence of nonmetallic inclusion or a surface defect which may be responsible for the formation of the micropit and it is assumed asperity interaction is responsible for eventual transfer. Each micropit is a distinct entity not necessarily connected in any way to the neighboring micropits. There are many microcracks present on the unpitted surface on this micrograph, e.g., at "C." The skid marked areas are regions where extensive micropitting has occurred and prolonged operation of the bearing in this condition would result in the progressive loss of material in the skid marked areas.

A smooth, non-skid marked area shown in Fig. 9 has a few extremely small micropits marked "A" which are not resolvable with the lower power microscope (30×). Some fine cracks at "B" are visible in various places of the nonskid marked area but they are well scattered and it does not appear that extensive micropitting is imminent in this area. However, while the area is not significantly damaged yet, comparing a noncontact surface (Fig. 7) and a nonskid marked area in a contact zone (Fig. 9), shows that some damage has taken place to the surface in the contact area. This is evidenced by the presence of microcracks in Fig. 9.

The surface studies previously described show that the skid marks are a surface phenomenon where micropits form over large areas. Sections cut from skid marked areas on inner rings were polished and etched for metallographic examination. Figure 10 is a photomicrograph showing the microstructure at a skid marked area. The white etching bands marked on the surface represent the remains of the original surface while the voids adjacent to

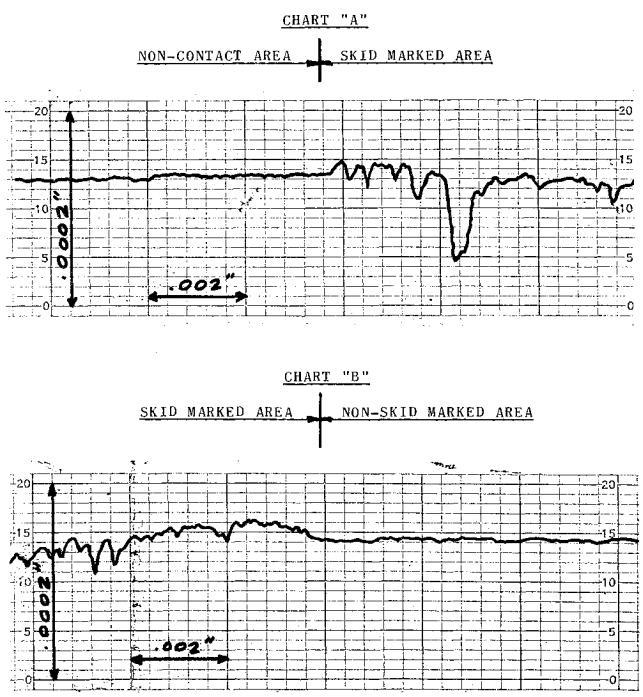

Fig. 6 Talysurf traces on skid marked bearings.

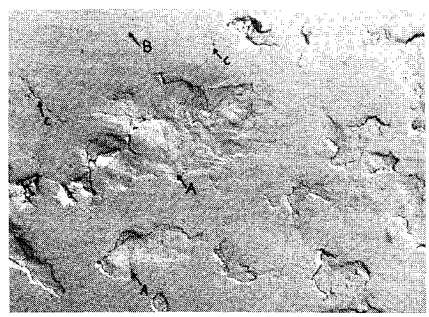

Fig. 8 Replica electron micrograph of skid marked region.

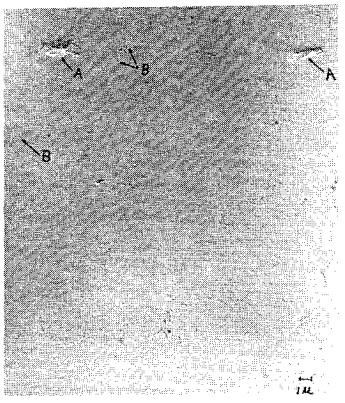

Fig. 9 Replica electron micrograph of nonskid marked region on contact surface.

the bands are the micropits. There is a correlation between the irregular surface seen in this picture and the Talysurf traces previously discussed. The depth of the micropits varies within the same limits as the thickness of the white bands in the photomicrograph. The white bands represent a new structure which formed during bearing operation. The original structure contained tempered martensite and spherical carbides as seen in the lower portions of the micrograph in Fig. 10. The white bands could conceivably consist of either rehardened or plastically deformed material or both. When the plastic deformation is carried too far and the durability of the material is exceeded, cracks will form which are seen in Figs. 8 and 9. The cracks form networks which result in micropitting or more properly microspalling. The depth of the pits corresponds to the depth of the plastically deformed layer. The cracks travel through the brittle deformed layer and stop at the boundary of this deformed layer because the material below is undeformed and more ductile. The crack then progates along the boundary between the deformed and undeformed material because this is the easy path for crack progation. Since plastically deformed layers are very thin, skid marks occur as a result of stresses in asperity dimensions and these nonshear stress depths are, in bearing surfaces, of the order of 100 μin.

Bearing Designs

When excessive slip is predicted, or examination of actual hardware shows evidence of skidding damage, the condition may be corrected by decreasing the number of rollers to increase the roller load, reducing the roller size to reduce the roller centrifugal forces, decreasing internal clearance to put more rollers under load if the ring and housing are relatively rigid and, in some cases, using a cage supported on the rotating ring. There are limitations, however, to such approaches and the most successful has been to increase the applied load on the bearing. A method of accomplishing this is to create a predetermined radial preload across the bearing through the configuration of the bearing components themselves; known as an "out-of-round" bearing illustrated by Given.[2] The configuration used to create the out-of-round conditions can either be bilobe or trilobe as shown in Fig. 11. It can readily be seen that with a bilobe bearing the two preload load zones are diametrically opposite each other which can create an unstable condition; whereas with the trilobe bearing, the preloads are applied 120° apart and results in a more stable bearing.

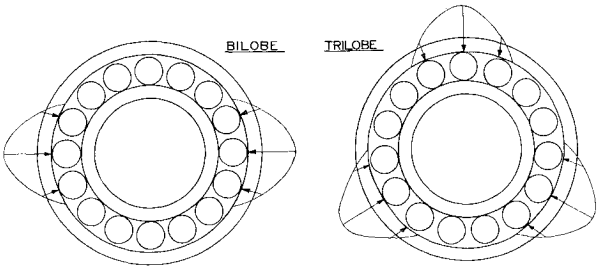

Fig. 11 Out-of-round designs.

Figures 12–14 illustrate the various out-of-round design methods to preload a bilobe bearing radially. These methods are also applicable to trilobe bearing. Method A in Fig. 12 shows a bearing with a cylindrical outer ring roller path and elliptical o.d. in the unmounted or free state. By inserting the outer ring in a round housing, the elliptical shape is transferred to the roller path, creating a preload across the bearing after mounting. The amount of preload is dependent upon the initial internal radial clearance in the bearing, the amount of out-of-round or wall section variation of the outer ring, the amount of average interference fit in the housing, and the relative stiffness of the housing and outer ring. In this case, as well as with other methods, the stiffness of the inner ring of the bearing and the shaft also effects the mounted preload to a minor extent.

Method B in Fig. 13 shows a bearing with an out-of-round outer ring and, in this case, a uniform wall section. In the free state the bearing is already internally preloaded with the magnitude dependent upon the initial out-of-roundness of the outer ring, the average internal radial

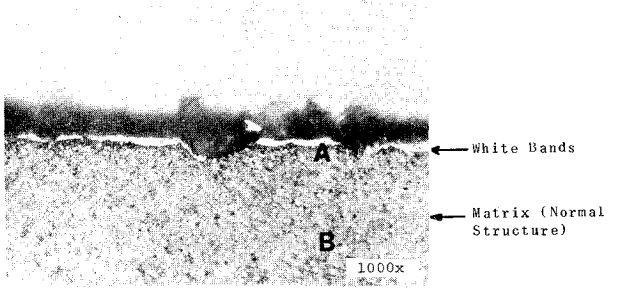

Fig. 10 Photograph of white bands at the surface of skid marked areas.

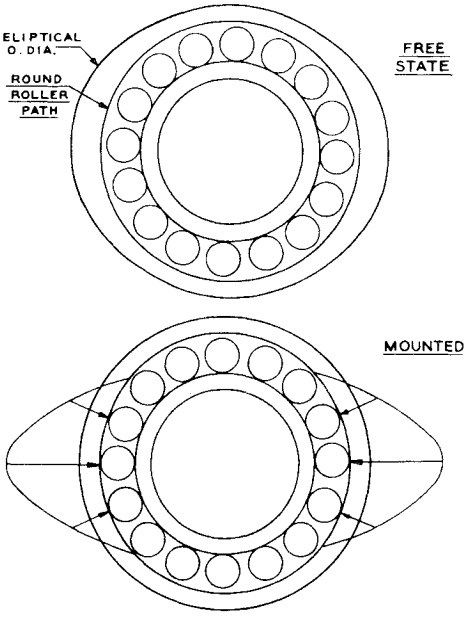

Fig. 12 Out-of-round design, method A.

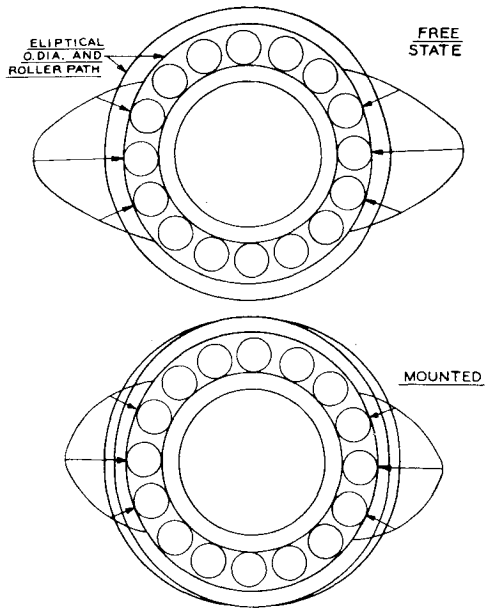

Fig. 13 Out-of-round design, method B.

clearance of the bearing, and the stiffness of the inner and outer rings. This design is also mounted in a round housing. If the housing fit has zero interference, the initial preload remains, but with an interference fit in the housing, the preload is relieved depending upon the amount of interference and the stiffness of the rings and mating parts. Because of the reduced conformity of contact between the outer ring and housing, antirotation pins or keys are generally used to prevent creep of the outer ring in the housing and subsequent wear or damage to the parts. Advocates of this method stress the importance of the clearance between the outer ring and the housing across the preload direction which provides a safety valve should the thermal difference between the inner and outer rings be

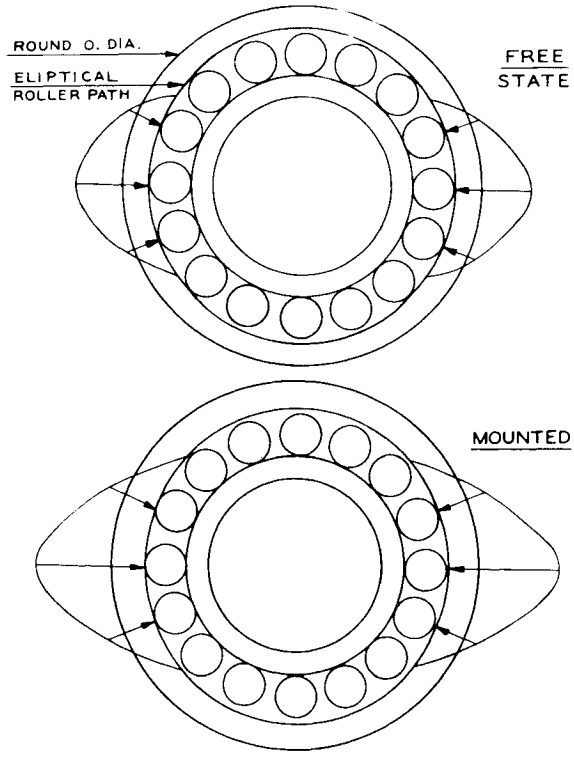

Fig. 14 Out-of-round design, method C.

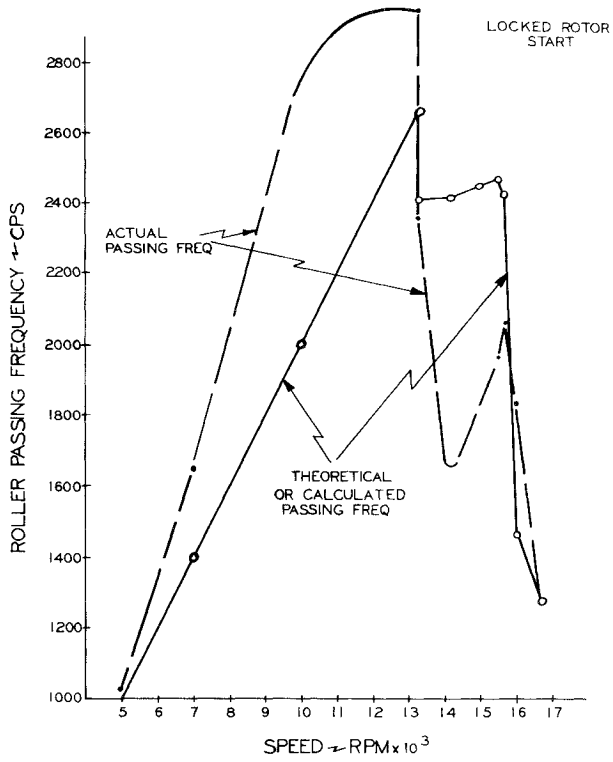

Fig. 15 Roller passing frequency vs speed.

underestimated and the inner ring expand excessively in operation.

Method C in Fig. 14, is a combination of the first two methods. The outer ring is manufactured with a cylindrical o.d. and an elliptical roller path. As in Method B, the bearing in the free state is initially preloaded with the magnitude dependent upon the initial out-of-roundness of the roller path, the average internal clearance in the bearing, and the stiffness of the rings. This design is also mounted in a round housing and an interference fit will further increase the initial preload with the magnitude dependent upon the stiffness of the bearing rings and mating parts. The advantage of this method over Method

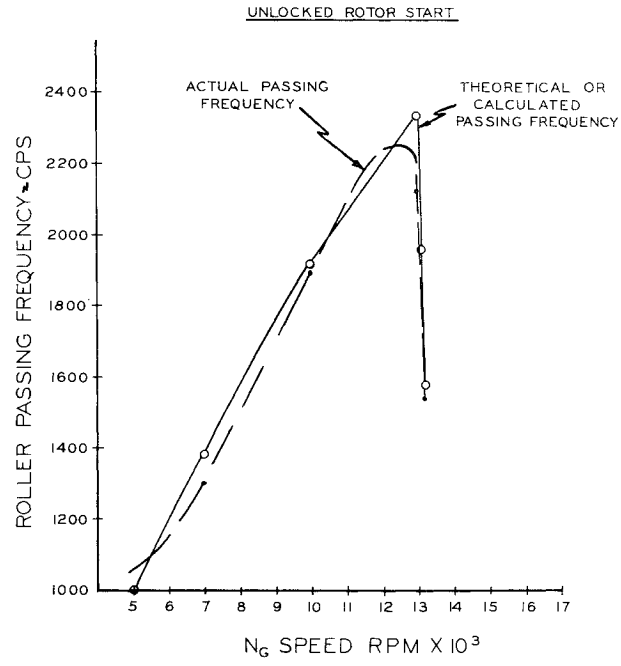

Fig. 16 Roller passing frequency vs N_G speed.

B is that a full conforming fit in the housing is achieved eliminating the necessity of pinning devices to prevent creep and fretting between the bearing o.d. and housing bore surfaces. The successful design of these preloaded bearings depends to a large extent on the internal clearance of the bearing after mounting and at temperature and speed, and the stiffness of the mating parts.

Slip in a Helicopter Engine

There are numerous successful aircraft engines and gear boxes in volume production with bearings operating quite successfully at high speeds and loads. However, the main shaft bearings used in a particular helicopter engine had been a continued source of trouble due to skidding damage. The operating conditions for the troublesome bearings are quite unique and different from the usual operating conditions. The usual operation is with a stationary outer ring and a rotating inner ring. In this particlar engine the outer ring rotates between 11,000–14,000 rpm with the inner ring stationary when the helicopter main rotor is in the locked position during ground operation. When the main rotor is unlocked the inner ring accelerates and rotates at 13,600 rpm with the outer ring rotating at speeds up to 18,000 rpm.

Early indications of a need to improve the bearing design was apparent when several bearings failed during ground testing of the helicopter. Since then several design changes, based on various failure theories, were evaluated in a factory and field testing program. The field testing program consisted of a tiedown test run by the airframe builders using normal and abnormal starting and steady-state operation. The bearing was instrumented to measure actual roller passing frequency which could then be compared to calculated values to determine if slip was occurring in the aircraft installation. Computer analysis predicted 82.5% slip with the rotor locked under less than 15 lb applied load and outer ring rotating at 14,000 rpm with a stationary inner ring. Engine and subsequent component testing verified the high slip. As a result of these tests it was concluded that: 1) bearing loads are very low during all phases of engine operation in the aircraft; 2) at rotor release there is a step function increase in bearing load; and 3) the cage and roller complement of normal open clearance bearings are subjected to rapid changes in speed during rotor release with subsequent damage to

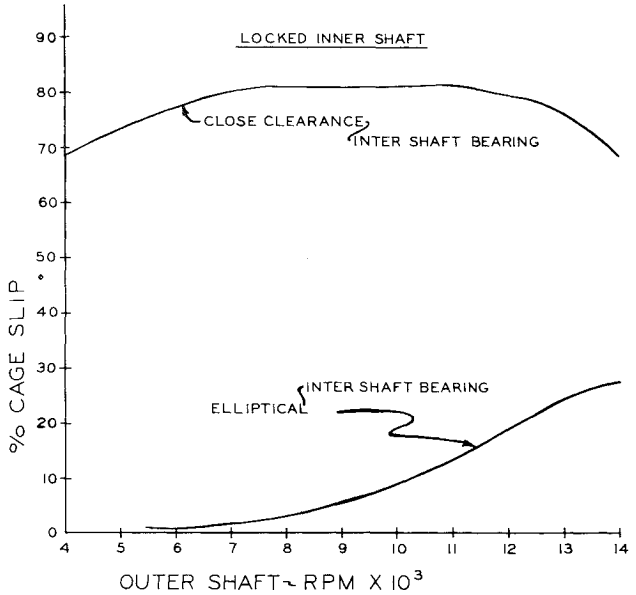

Fig. 17 Percentage cage slip vs outer shaftspeed.

In all tests, the stress data plots had the same characteristics; a very low load during gas generator start to idle, a sudden step increase in load at idle when the rotor brake was released, a gradual rise in load until gas generator rotor reached about 14,250 rpm, then a gradual decrease in load until gas generator rotor reached 16,250 rpm, and then a steady load to 100% speed. Typical dynamic loads are: 1) start to idle, locked rotor constant load of 4.5 lb; 2) load at idle after brake release 18.2 lb; and 3) load above idle with rotor turning, a) steady increase to 31.8 lb @ 14250 Ng, b) then steady decrease to 5.5 lb @ 16250 Ng. On engine starts with an unlocked rotor, loads during start to idle were about 3.7 lb. There was no significant increase in load at idle.

Based on a detailed review and analysis of the strain gage output signal wave shape for locked and unlocked rotor starts, the bearing cage speed could be determined. By analysis of plots of the cage speed, it has been determined that at the time of rotor release, there is a sudden change in cage speed. This change occurs as a rapid deceleration of the cage which, in turn, causes the rollers to slip on the inner and outer races inducing roller and race skid damage. This damage accumulates on each rotor release and in a short period of time causes bearing distress. Actual test results are shown in Figs. 15 and 16.

Discussions regarding ways of reducing the drag forces or increasing the driving forces were held. Such modification as lubrication, internal bearing design, and material were evaluated. Since the bulk lubricant itself can provide a drag force, consideration was given to the effect that lubricant temperature and flow rate would have on slip. Test results show that increasing the oil flow or decreasing the oil temperature increases slip. Low oil flow can reduce slip but may increase skidding damage. This may be due to a thermal phenomena or starvation at the contacts. The low oil flow is insufficient to create an effective EHD film resulting in increased metal to metal contact and increased temperature at the raceway contacts. Thus, the rings begin to expand tending to load more rollers and reduce slip but the increase in temperature also lowers the lubricant viscosity which results in a lower lubricant film thickness failing to keep the contacting surfaces separated.

The first modification to the bearing design to reduce slip was to reduce the radial clearance by approximately 50%. Although the tighter clearance required less load to reduce slip, skidding damage was not eliminated. Next an elliptical bearing design study using the SKF computer program was conducted to choose an ellipticity to give proper preload and still have good fatigue life. The radial clearance selected was adequate to insure that the ellipticity of the outer ring o.d. and roller path (Fig. 13) would preload the rollers and maintain at least 20% of the rollers in the loaded zone. A loose fit on the outside diameter was used to allow the elliptical outer ring to flex and to insure that the housing fit did not remove the ellipticity. With this arrangement a key type retaining ring was used to prevent the outer ring from rotating in the housing. The recommended and evaluated ellipticity was 0.022 in. Test data with the elliptical bearings are shown in Fig. 17, indicating the cage slip was substantially reduced (approximately 80% for the standard bearings to 30% with an elliptical bearing). Substantial testing of the elliptical bearing has been completed with no apparent problems.

Other bearing design changes such as cage design and reduced roller complement were evaluated but did not reduce the slip to an acceptable level. The tests were repeated for comparison between the standard bearing with reduced radial clearance and an elliptical bearing. The elliptical bearing showed no sign of skidding damage. However, CVM M-50 material was recommended as a safeguard improvement because it was found experimentally superior and this may be due to higher temperatures.

The results of these tests and many others show that for lightly loaded, high-speed aero/space applications where slip is resulting in skidding damage the elliptical, preloaded bearing should be considered as a viable solution. There are thousands of engines both in military and commercial planes as testimonial for the success of the elliptical preload principle.

Conclusion

While the out-of-round concept has proven itself adequate in many engine applications of all major engine builders, it has not been without problems. In recent years, and as late as this past fall, both intershaft bearings and main shaft bearings have all had roller/raceway skid problems with elliptical bearings. This points out that though we have a fundamental analytical tool to predict roller slip, there is no detailed understanding of the conditions at which damage results when slip occurs. Under extremely stable lubrication and operating conditions considerable slip may occur without surface damage. However, under unfavorable lubrication conditions the thermal or mechanical shock of the slip can collapse, or cause total or partial absence of oil film with resulting surface damage. A predictive criterion is not available to predict when skid damage will occur.

In order to permit design optimization of cylindrical roller bearings to prevent skid damage, a more analytical program is needed to 1) improve prediction of lubricant film conditions using more up-to-date lubrication models, and 2) determine a damage criterion for roller/raceway contacts and use it to predict regimes in which skid damage may occur.

References

[1]Harris, T., "An Analytical Method to Predict Skidding in High Speed Roller Bearings," *ASLE Transactions* (American Society of Lubrication Engineers), Vol. 9, 1966, pp. 229–241.

[2]Given, P. S., Main Shaft Preloaded Roller Bearings "State of the Art—Bearing Technology," presented at the ASME Winter Annual Meeting, Chicago, Nov. 1965.

APRIL 1975 J. AIRCRAFT VOL. 12, NO. 4

Solid Lubricated Bearing Inter-Element Heat Transfer Mechanisms

Darryl E. Metzger*
Arizona State University, Tempe, Ariz.

Solid lubricated bearings suffer from the absence of a good heat transfer medium such as provided in conventional bearings by the lubricated oil. The frictional heat generated in localized areas in the bearing produces large temperature gradients, some of them periodic, which undoubtedly contribute to failure. A need exists for better knowledge of the internal heat transfer between bearing elements to aid in accurate computation of the element temperature distributions. In this paper, results are reported for a series of experiments made with actual bearings, both annular and pellet separator types, to explore the characteristics of the heat transfer occurring within the bearing operating in an air environment. Measured element temperatures reveal a strong propensity of the bearings to isolate themselves from the adjacent ambient air. Overall ring-to-ring conductances are evaluated from the measured temperatures and electrically imposed heat fluxes. The separate roles of convection and conduction are explored with tests on modified bearings and with a tentative model of the transient conduction at the ball-raceway contact.

Nomenclature

A	= inner surface area of the outer bearing ring
k	= thermal conductivity
l	= length of ball-race contact ellipse
N	= bearing speed
$\dot{q}, \dot{q}_{r,o}$	= electrically supplied heat transfer rate
$\dot{q}_1, \dot{q}_2, \dot{q}_3$	= thermal circuit heat transfer rates (see Fig. 6)
R_1, R_2, R_3	= thermal circuit resistances (see Fig. 6)
$s_b, s_{r,o}$	= frictionally generated energy rate (see Fig. 6)
t_b	= bearing ball temperature
t_p	= bearing pellet temperature
$t_{r,i}$	= bearing inner ring temperature
$t_{r,o}$	= bearing outer ring temperature
t_s	= bearing annular separator temperature
U	= thermal conductance
w	= width of ball-race contact ellipse
α	= thermal diffusivity
θ	= ball-race contact time

Received July 22, 1974; revision received November 14, 1974. This study was supported by contract from the Air Force Aero Propulsion Laboratory through the AiResearch Manufacturing Company.

Index category: Thermal Modeling and Experimental Thermal Simulation.

*Professor and Chairman of Mechanical Engineering; also Consultant, AiResearch Manufacturing Company, Phoenix, Ariz. Member AIAA.

Introduction

TYPICAL rolling element bearing applications in gas turbine engine technology utilize a continuous recirculating oil flow for both lubricating and cooling purposes. There are many instances, however, where the necessary complexity of the oil system and the requirement of relatively low oil temperatures make the conventionally lubricated bearing quite unattractive. A possible alternative, particularly for applications which require a relatively short service life but long unattended shelf life, is the solid lubricated bearing where the lubricant is contained within the bearing in a solid, wearable element.

The service life of bearings, like most machine components, is in part dictated by the operating temperature distribution, especially when the temperature gradients are large and periodic. In conventionally lubricated bearings, a major function of the oil, in addition to providing the lubricant film, appears to be its ability to remove heat rapidly from the localized contact where frictional heat generation occurs. The oil not only removes the generated energy from the bearing; but in the process redistributes thermal energy among the bearing components, reducing the temperature gradients.